03

# Postponing transition to turbulence in the swept wing boundary layer by means of stationary disturbances control using plasma actuator

© A.Ya. Kotvitskii[1], A.A. Abdullaev[1,2], M.V. Ustinov[3], I.A. Moralev[1]

[1] Joint Institute for High Temperatures, Russian Academy of Sciences, Moscow, Russia
[2] Moscow Institute of Physics and Technology (National Research University), Dolgoprudny, Moscow Region, Russia
[3] Zhukovsky Central Aerohydrodynamic Institute, Zhukovsky, Moscow oblast, Russia
E-mail: morler@mail.ru

*Received February 26, 2025*
*Revised March 19, 2025*
*Accepted March 19, 2025*

Control of a laminar-turbulent transition, driven by cross-flow instability in a swept wing boundary layer, is attempted using close-loop suppression of natural stationary disturbances. To fulfill this task, a control system based on multichannel plasma actuator, particle image velocimetry- base sensor and controller was designed and built. Control was based on the closed -loop optimization of the actuator voltages, implemented by gradient descent algorithm. Control was implemented for the stationary cross-flow vortices excited by isolated roughness on the plate surface. Reduction of the disturbances amplitude was achieved, with a significant downstream shift of the transition region.

**Keywords:** feed-backward control, plasma actuator, flow control, barrier discharge, boundary layer.

DOI: 10.61011/TPL.2025.06.61297.20297

It is an important challenge in aerodynamics to delay the transition to turbulence or increase the extent of the laminar flow zone around the wing surface and the empennage of an aircraft. It is known that laminarization of flow around the leading edge of the wing surface of a medium-range aircraft helps reduce the fuel consumption by 10% [1]. Laminar airfoils with a long flow acceleration section, which eliminates instability with respect to Tollmien–Schlichting waves, do not provide a profit in the case of a swept wing. This is caused by a specific type of instability of a three-dimensional boundary layer that forms in the region of a negative pressure gradient and is caused by the presence of a velocity component transverse to the external flow line (the so-called cross flow) within the boundary layer [2–4]. The cross-flow instability modes are vortices with their axes being nearly parallel to the external flow line. At low levels of turbulence, these vortices are generated by irregularities on the wing surface and do not shift their position over time. The transition to turbulence is induced by secondary high-frequency instability of the boundary layer modulated by stationary vortices of cross-flow instability. Secondary high-frequency instability develops when the amplitude of the primary disturbances in the boundary layer reaches $\sim 30\%$ [5]. This is the reason why the section of nonlinear development of disturbances is long (compared to the two-dimensional case), possibly extending to tens of percent of the wing chord.

Known methods for delaying the transition to turbulence on a swept wing involve altering the velocity profile in the boundary layer with surface relief [6] or a volumetric force [7,8] and modulating the boundary layer with short-period instability vortices, which are induced by irregularities at the leading edge of the wing [3,9,10]. In addition, laminarization by means of boundary layer suction remains efficient in the case of a swept wing (just as in a two-dimensional boundary layer) [2].

Reactive methods of counter-phase disturbance control, such as wave cancellation, are potentially more energy efficient than modification of the boundary layer velocity profile. Such approaches have been implemented for various flows and types of disturbances: Tollmien–Schlichting waves in two-dimensional boundary layers [11], Kelvin–Helmholtz instability in turbulent jets [12,13], etc. The main idea of wave cancellation is to obtain „natural“ disturbances with a system of sensors and introduce control disturbances by an actuator. Linear combination of these disturbances with natural waves provide a reduced amplitude of oscillations or velocity modulation in the boundary layer. The capacity to measure „natural“ disturbances accurately is critical for the realization of this method. This means that sensors need to be placed far enough from the leading edge where the disturbances have a sufficient amplitude. When stationary or narrow-band non-stationary disturbances are used for control, actuators may be positioned upstream from the sensor, which provides a high gain for the control disturbances. This is useful, since the maximum amplitude of modes generated by actuators is often limited.

The operation of such a system for control over the transition caused by cross-flow instability was investigated theoretically in [14]. It was demonstrated that efficient suppression of arbitrary „natural“ disturbances may be achieved if the spatial resolution of actuators and sensors of the system in the transverse direction does not exceed a

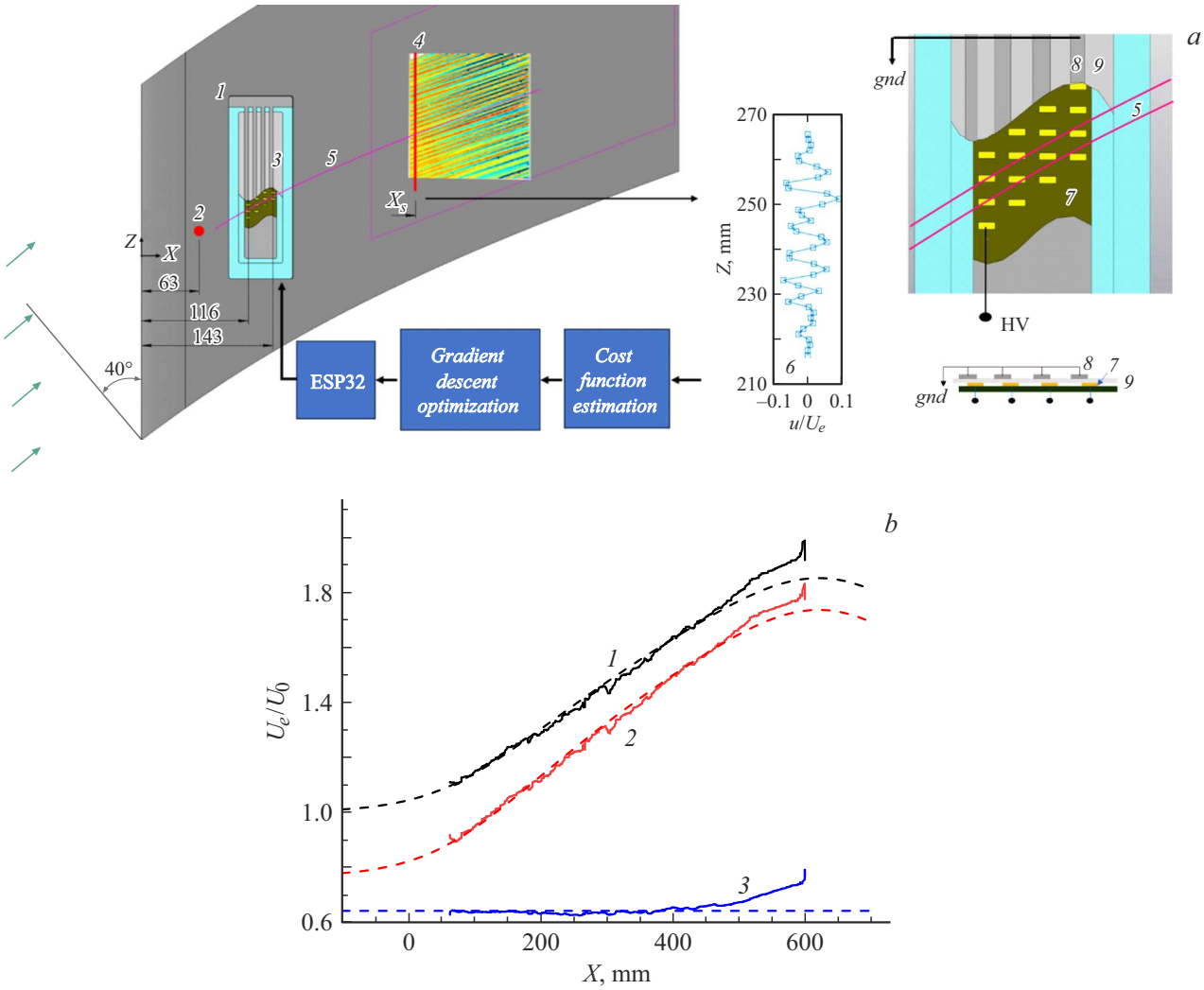


**Figure 1.** *a* — Experimental setup and plasma actuator design. *1* — Plate, *2* — irregularity, *3* — actuator, *4* — velocity field measurement (PIV) region, *5* — constant phase lines for stationary disturbances with a wavelength of 7 mm, *6* — transverse profile of local velocity in the boundary layer $u(Z)$, *7* – control (high-voltage) electrodes, *8* — common exposed electrode, and *9* — ceramic layer. *b* — Dependences of the following characteristics of external flow on $X$: velocity at the upper boundary of the boundary layer $U_e$ (*1*) and its $X$-axis (*2*) and $Z$-axis (*3*) components. Solid and dashed curves correspond to measured and calculated data.

quarter of the period of the instability mode that grows the fastest. Various devices (barrier discharge systems included) may be used as actuators. Excitation of the boundary layer on a swept wing by plasma actuators was studied in detail in [15–18]

In the present study, we implement stationary instability vortex control in an artificial flow simulating a boundary layer on a swept wing. The experiment was conducted in a D-3 wind tunnel at the Joint Institute for High Temperatures of the Russian Academy of Sciences. The test section was 300 × 300 mm in size, and the level of flow turbulence at the entrance to the test section was 0.06 %. The diagram of the experiment is shown in Fig. 1, *a*. The boundary layer was formed on a flat plate positioned horizontally in the working section of the tunnel. The elliptical leading edge of the plate was inclined at a sweep angle of 40° to the incoming flow. To produce a pressure gradient normal to the leading edge of the plate, the upper wall of the test section of the wind tunnel was profiled. The side walls of the working section were also profiled according to the shape of the near-wall streamlines in order to maintain a uniform span-wise distribution of flow parameters. The coordinate system with axes $X$, $Z$ bound to the swept leading edge of the model is used below to analyze the experimental data. The flow acceleration region length was $L = 610$ mm. The experiment was carried out at incident flow velocity $U_0 = 25$ m/s, atmospheric pressure, and room temperature; these parameters correspond to Reynolds number $\mathrm{Re}_L \sim 10^6$. The dependences of the absolute value and velocity components of the external flow velocity above the boundary layer on the longitudinal coordinate are shown in Fig. 1, *b*. Their uniformity

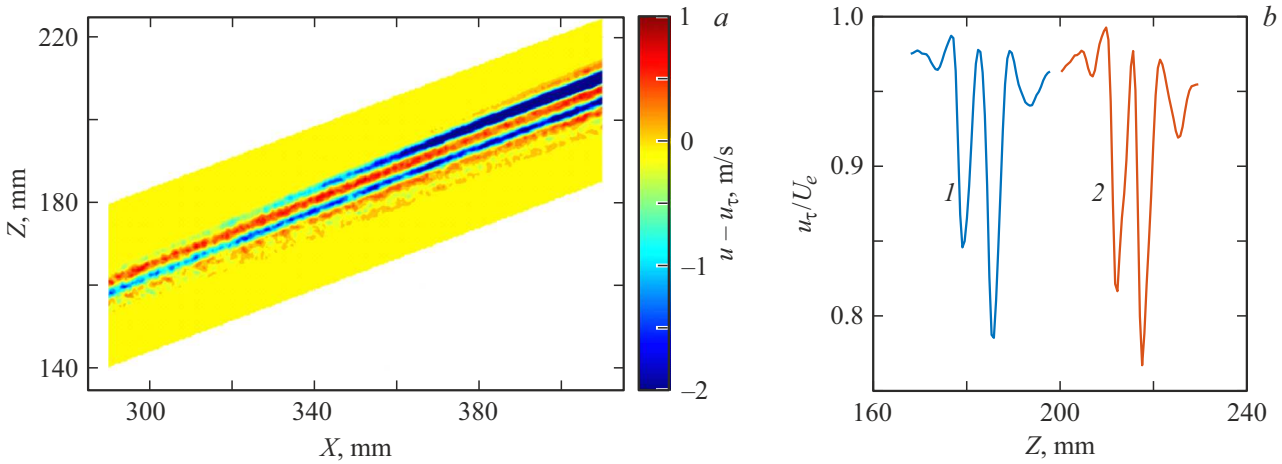


**Figure 2.** *a* — Stationary instability vortices induced by a single actuator section at a supply voltage amplitude of 4 kV. *b* — Profile of velocity along the plate surface $u_\tau$ at distance $X = 300$ mm from the leading edge and a height of 1 mm from the wall. *1* — Behind the roughness element; *2* — behind the discharge.

in magnitude in the central part of the model with a width of 150 mm and the slip condition (constancy of the transverse velocity component along the longitudinal coordinate) were preserved down to $X = 470$ mm. The characteristic boundary-layer displacement thickness ranged from 0.45 to 0.6 mm, and the maximum value of the cross-flow velocity in the boundary layer was 8 % of the velocity at its outer boundary. Calculations of the boundary layer stability revealed that the transverse period (along the $Z$ axis) of the fastest growing stationary disturbances is close to 7 mm under the conditions of the present experiment [14]. Disturbances in the boundary layer were recorded using a particle image velocimetry (PIV) system, which measured the velocity field at a frequency of 7 Hz with a resolution of 0.15 mm. Measurements were carried out in a plane located at a height of approximately 1–1.3 mm above the surface of the plate and parallel to it. It should be noted that the chosen height exceeds slightly the one at which the maximum amplitude of velocity modulation in the cross-flow instability vortices is achieved (approximately 0.7 mm, or 1.5 times the boundary-layer displacement thickness).

A multichannel actuator based on barrier discharge (Fig. 1, *a*) was used to excite the boundary layer. Its electrodes were located at distance $X = 116-146$ mm from the leading edge of the model. This actuator was composed of a dielectric plate with four metal grounded electrodes glued onto its streamlined surface, with their edges parallel to axis $Z$. High-voltage electrodes arranged in four rows of four electrodes each were mounted under the surface of the dielectric. Electrodes of different rows were shifted relative to each other along the leading edge in such a way as to form an array of pointwise disturbance's sources with a uniform pitch of 1.7 mm on the line perpendicular to the axes of vortices. This design, on the one hand, provides the required spatial resolution and, on the other hand, minimizes the mutual influence of actuator channels. The discharge was initiated on the surface of an alundum plate with a thickness of 0.5 mm. AC voltage with an amplitude up to 5 kV and a frequency of approximately 80 kHz was applied individually to each of the high-voltage electrodes; its amplitude was set proportionally to the control signal. The characteristic volumetric force produced in the vicinity of the corona electrode was determined in [19] and was on the order of 1.5 $\mu$N per channel. A system combining a personal computer with an ESP32 microcontroller was used to control the actuator.

The gradient descent algorithm was used to choose the optimum distribution of voltage over the actuator channels. The root-mean-square amplitude of modulation of the time-averaged velocity in a cross section located at a distance of 300 mm from the leading edge of the plate was chosen as the cost function. At each step of the algorithm, the flow velocity profile along transverse coordinate $Z$ was measured, the value of the cost function was calculated, and the voltage at one of the actuator channels was varied. With all 16 channels checked, the cost function gradient was calculated, and the next step of the algorithm was implemented. On average, the cost function was minimized in 5–9 iterations.

Figure 2, *a* shows stationary disturbances of the longitudinal velocity component induced by a single actuator section in the boundary layer. They take the form of alternating bands of low and high velocity streaks induced by the transfer of longitudinal momentum in the boundary layer by cross-flow instability vortices. A comparison of disturbances from a single discharge and an isolated roughness element of a small width (Fig. 2, *b*) reveals that the structure of the vortex packet from these two disturbances at the same distance from the leading edge are similar.

Figure 3 presents the results of controlling the transition to turbulence behind a single cylindrical element with a diameter of 3 mm and a height of 200 $\mu$m located at distance $X = 70$ mm from the leading edge of the model. Without

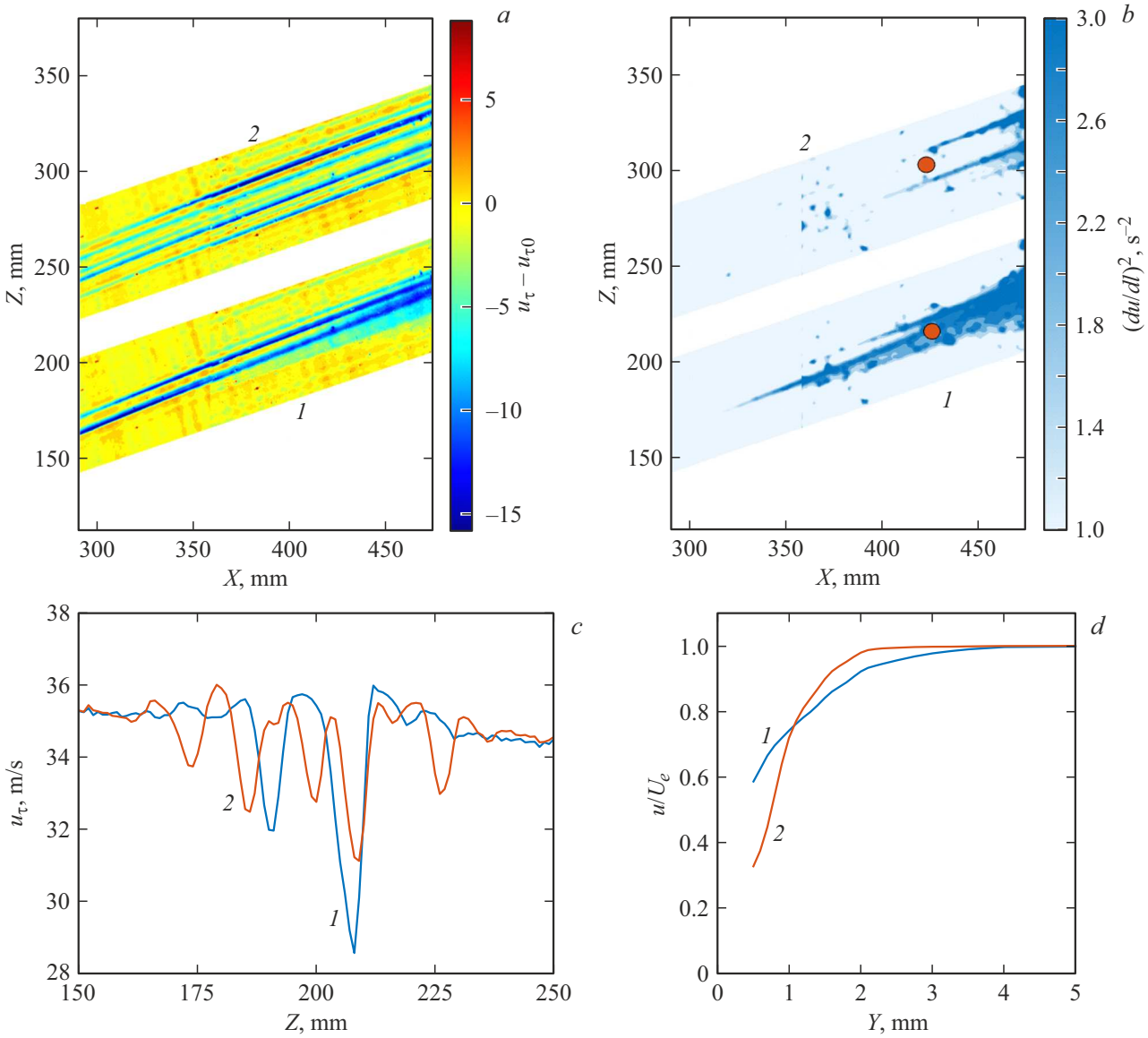


**Figure 3.** *a* — Velocity field at a distance of 1.3 mm from the plate; *b* — amplitude of short-period velocity pulsations in the same cross section; *c* — transverse velocity profile in the boundary layer at distance $X = 300$ mm from the leading edge and a height of 1 mm from the plate; and *d* — average velocity profiles in the boundary layer in the region marked in panel *b*. *1* — Without control; *2* — after optimization of the voltage distribution at the electrodes.

control, a packet of instability vortices forms behind the element (Fig. 3, *a*), producing a turbulent wedge at distance $X = 310$ mm from the leading edge (Fig. 3, *b*). The laminar-turbulent transition line is visualized by the distribution of amplitude of short-period (with a wavelength shorter than 4 mm) velocity pulsations. Such disturbances correspond physically to high-frequency pulsations associated with secondary instability or arise in the turbulent flow regime. Sequential optimization of the voltage distribution over the actuator channels allows one to induce a significant downstream shift of the turbulent wedge tip. This is achieved by suppressing two vortices that form behind the irregularity (Fig. 3, *c*). A packet of disturbances with a smaller amplitude and a wavelength on the order of 4–5 mm is formed instead of them in the boundary layer. The characteristic shift of the turbulent wedge tip in the considered experiment is up to 100 mm (or approximately 25% of the initial length of the laminar flow region behind the roughness element. The vertical velocity profiles averaged within the regions circled in Fig. 3, *b* are shown in Fig. 3, *d*. It can be seen that when artificial disturbances created by the discharge interfere with natural vortices generated by the irregularity, the velocity profile becomes less filled. This verifies the assumption of flow laminarization.

Thus, the delay of the transition to turbulence in a three-dimensional boundary layer, which imitates the boundary layer on a swept wing, through antiphase suppression of

natural disturbances in the feedback mode was demonstrated experimentally. A plasma actuator design establishing control with a transverse resolution of approximately 1.7 mm, which corresponds to a quarter of the period of the fastest growing disturbances in the discussed experiment, was proposed.

### Funding

This study was supported financially by the Russian Science Foundation (grant No. 24-19-00627).

### Conflict of interest

The authors declare that they have no conflict of interest.

## References

[1] G. Schrauf, Aeronaut. J., **109**, 639 (2005). DOI: 10.1017/S000192400000097X
[2] H. Bippes, Prog. Aerosp. Sci., **35**, 363 (1999). DOI: 10.1016/S0376-0421(99)00002-0
[3] W.S. Saric, H.L. Reed, E.B. White, Annu. Rev. Fluid Mech., **35** (1989), 413 (2003). DOI: 10.1146/annurev.fluid.35.101101.161045
[4] Y.S. Kachanov, Annu. Rev. Fluid Mech., **26**, 411 (1994). DOI: 10.1146/annurev.fl.26.010194.002211
[5] M.V. Ustinov, Y.S. Kachanov, Phys. Fluids, **33** (9), 094105 (2021). DOI: 10.1063/5.0057853
[6] D.A. Mischenko, A.V. Ivanov, M.V. Ustinov, AIP Conf. Proc., **2027**, 030152 (2018). DOI: 10.1063/1.5065246
[7] S. Yadala, *Control of stationary crossflow instability using DBD plasma actuators* (Delft, 2016). https://resolver.tudelft.nl/uuid:3db8e948-1fb8-4390-a117-3b5eaae8cb83
[8] P.C. Dörr, M.J. Kloker, J. Phys. D, **48** (28), 285205 (2015). DOI: 10.1088/0022-3727/48/28/285205
[9] S. Yadala, M.T. Hehner, J. Serpieri, N. Benard, M. Kotsonis, in *2018 Flow Control Conf.* (Atlanta, Georgia. 2018), AIAA 2018-3215. DOI: 10.2514/6.2018-3215
[10] R. Radeztsky, M. Reibert, W. Saric, in *Fluid Dynamics Conf.* (Colorado Springs, CO, 1994), AlAA-2373. DOI: 10.2514/6.1994-2373
[11] A.S.W. Thomas, J. Fluid Mech., **137**, 233 (1983). DOI: 10.1017/S0022112083002384
[12] D.B.S. Audiffred, A.V.G. Cavalieri, I.A. Maia, E. Martini, P. Jordan, J. Fluid Mech., **994**, A15 (2024). DOI: 10.1017/jfm.2024.569
[13] V.F. Kopiev, O.P. Bychkov, V.A. Kopiev, G.A. Faranosov, I.A. Moralev, P.N. Kazansky, Acoust. Phys., **67** (4), 413 (2021). DOI: 10.1134/S1063771021040059
[14] A. Abdullaev, A. Kotvitskii, I. Moralev, M. Ustinov, Aerospace, **10** (5), 469 (2023). DOI: 10.3390/aerospace10050469
[15] J. Serpieri, S.Y. Venkata, M. Kotsonis, J. Fluid Mech., **833**, 164 (2017). DOI: 10.1017/jfm.2017.707
[16] S. Yadala, M. Hehner, J. Serpieri, N. Benard, M. Kotsonis, AIAA J., **59** (9), 060101 (2021). DOI: 10.2514/1.J060101
[17] K.-S. Choi, J.-H. Kim, Exp. Fluids, **59** (10), 159 (2018). DOI: 10.1007/s00348-018-2609-x
[18] S. Baranov, I. Moralev, M. Ustinov, D. Sboev, S. Tolkachev, in *Proc. 593 Euromech. Colloqium Plasma-based actuators for flow control: recent developments and future directions* (Delft, Netherlands, 2018).
[19] I. Moralev, V. Bityurin, A. Firsov, V. Shcherbakova, I. Selivonin, M. Ustinov, Proc. Inst. Mech. Eng. G, **234** (1), 42 (2020). DOI: 10.1007/10.1177/0954410018796988

*Translated by D.Safin*